Dynamics and acoustics of a spherical bubble rising under gravity in an inviscid liquid

Giorgio Riccardi[a)]

Department of Industrial and Information Engineering

Second University of Naples

I-81031 Aversa, Italy

and

Enrico De Bernardis[b)]

Marine Technology Research Institute

National Research Council of Italy

I-00128 Rome, Italy

[a)]Also at: Marine Technology Research Institute, National Research Council of Italy, I-00128 Rome, Italy.

[b)]e-mail: enrico.debernardis@cnr.it.

Abstract

The rising motion and the acoustic emission of a pulsating spherical gas/vapour bubble in an isochoric, inviscid liquid are investigated. The motion is driven by the uniform and constant force field due to the gravity. The liquid is assumed at rest at the initial time. Unlike previous work on this subject, the mass of the bubble is not neglected, so that the bubble motion is accurately simulated also in the presence of large volume variations. After developing the relationships between the bubble motion to the liquid flow, a system of two nonlinear ODEs for the radius and the position of the center of mass of the bubble is written. The near-field pressure disturbance produced in the liquid by the bubble motion is evaluated by means of elliptic integrals and an efficient approximation of it free from these special functions is also used. The numerical integration of the ODE system allows to evaluate the acoustic signal. This is carried out with the above mentioned approximation, and several features of it are demonstrated through the study of a sample flow.

I. INTRODUCTION

The phenomenon of cavitation is, in many cases, a critical issue for the hydrodynamic performance of the propulsion system of a ship, as well as for the thereby radiated noise. Along with a large effort in the development of CFD codes, aimed at improving the capability of simulating multiphase flows, significant work is devoted within the fluid dynamics community to achieve more insight in cavitation through accurate modeling of the relevant bubble dynamics (Brennen, 1995). Crucial points are the motion of the bubble as a whole and the evolution of its volume in connection with the pressure field in the surrounding liquid.

Over the last twenty years a number of papers were devoted to several aspects of the evolution of gas (and vapour) bubbles moving within a liquid. In the following are mentioned contributions aimed at improving understanding of the interaction between the translating motion of a bubble and the simultaneous variation of its size.

A first group of papers deal with the coupled dynamics of a bubble moving under the effect of pressure gradient due to a forcing acoustic pressure field. It is well represented by papers of Reddy and Szeri (2002a,b), and Doinikov (2002, 2004). In all of the above papers the radial motion of the bubble is determined through a form of the Rayleigh-Plesset equation, somehow corrected to take into account the compressibility of liquid. In Reddy and Szeri (2002a) a model derived by Magnaudet and Legendre (1998) is used in order to write the equation for the translating motion coupled with that for radial dynamics of the spherical bubble. In Reddy and Szeri (2002b) the same system of equations is perturbed, following a method proposed by Plesset (1954), to study the stability of spherical shape

under the coupling with translational motion. In Doinikov (2002) both equations are derived using a Lagrangian formulation, and then correction for liquid compressibility are applied to the equation for radial motion in the form proposed by Keller and Miksis (1980). In Doinikov (2004) the mutual interaction of volume pulsation, translational motion and shape oscillation (the two latter assumed to be small) is studied, by expanding surface modes in a series of Legendre polynomials, obtaining coupled equations to the second order in the interaction terms. Shaw (2006) extends the analysis of Doinikov (2004), by including third order interactions in the bubble axial velocity and shape modes, to demonstrate how the interaction of shape modes can affect bubble motion and volume oscillation. In all cases the ratio of the densities of fluid inside and outside the bubble does not play any role, that is the density of the bubble is neglected.

A second group of works deals with the problem (not considered here) of the interaction between shape oscillation and translating motion of a bubble rising due to the gravitational force. Yang *et al.* (2003) investigate the rectilinear rise of a bubble undergoing a transient behavior: the evolution of the bubble shape from release to steady state is numerically simulated, while the ascent of a bubble which expands, or contracts, due to a change in the ambient pressure is analytically studied. Klaseboer and Khoo (2006) study the effect of the presence of solid walls near the bubble, along with the effect of gravity. To do so they introduce equivalent bubble radius and wall velocity to extend the solution of Rayleigh-Plesset equation to the case of a rising non-spherical bubble. Gordillo *et al.* (2012) compared the results of their theoretical model of a rising bubble with the shape deformation numerically simulated by means of a Navier-Stokes code.

Finally, in Tuteja *et al.* (2010) the motion of a spherically pulsating gas bubble under

gravity in an inviscid fluid is investigated, based on developments from previous work (Chakraborty, 1990; Chakraborty and Tuteja, 1993), where the Lagrange formalism was used to derive the equations of motion. The study is focused on the effects of changing gravity on the bubble motion in a vertical plane. Tuteja *et al.* (2010) is the closest reference to the work presented here: when the horizontal component of the velocity of the center of mass is set to zero, the model reduces to one describing the vertical motion of the bubble coupled with the spherical pulsation of its surface. The density of the bubble is neglected in the comparison with that of the displaced liquid.

Significant effort has been spent to study the noise emissions from bubbles. Outstanding contributions come from experimental investigation of specific problems in practical applications as, for example, some works of Ceccio (Ceccio and Brennen, 1991; Choi and Ceccio, 2007; Chang and Ceccio, 2011). Despite a deep interest in cavitation noise, it is quite difficult to find experimental data for freee-space far-field acoustics of a single rising bubble. So, illustrating the features of the model presented here mostly rely on theoretical arguments, for which a suitable reference is found in the conceptual developments of Leighton (1994). Comparison with an experiment is proposed at the end, where the acoustic far-field of the rising bubble has been calculated in conditions derived from the data of a famous paper by Strasberg (1956).

In the present paper, dynamics and acoustics of a spherical gas/vapour bubble rising in an isochoric, inviscid liquid are investigated. In Section II a system of two nonlinear ODEs describing the dynamics of the spherical bubble is deduced, by relating the velocity potential in the liquid with the bubble motion induced by the gravity field. A modified form of the Rayleigh-Plesset equation describes the evolution in time of the bubble radius,

while the other equation gives the position of the center of mass during the rising motion. Both equations are nonlinearly coupled and, unlike all papers referenced above, the ratio of the densities inside and outside the bubble is taken into account as a parameter of the model, and it is shown to be meaningful in certain conditions. In Section III, according to a solution proposed by Farassat (2007) to the equation of Ffowcs Williams and Hawkings (1969), the near-field pressure generated in the liquid is evaluated by means of elliptic integrals and an efficient approximation of it, free from these special functions, is used instead. It is based on a Maclaurin expansion in the ratio between the bubble radius and the distance between observer and center of mass of the bubble. The bubble motion and the related (approximation of) acoustic disturbance are numerically evaluated in Section IV, where a comparison is made with the signature generated by a bubble formed at the release of air from a nozzle in water, illustrated in a famous paper on the subject (Strasberg, 1956). Some qualitative aspects of the dynamics and acoustics of the rising bubble are illustrated in sample flows. Finally, conclusions are offered in Section V, together with a brief description of the future work.

II. EQUATIONS OF MOTION OF THE SPHERICAL BUBBLE

The bubble, shown in Figure 1, is assumed spherical at any time and its center of mass is thought of as superimposed to the center of the sphere. The radius (R) and the position of the center of mass ($\boldsymbol{x}_{\mathrm{cm}}$) of the bubble depend on time (t). They are solution of a second order Cauchy differential problem that will be written below. Inside the bubble there is a gas/vapour mixture which does not diffuse across the bubble boundary and is subjected to isothermal compressions, $R(t) < R_0$, or expansions, $R(t) > R_0$, R_0 being the

radius at the initial time ($t = 0$). The surrounding liquid is homogeneous, inviscid and moves in an isochoric way, *i.e.* its density ρ is constant in space and time. It is assumed at rest at the initial time, therefore its motion remains irrotational at any successive time. On the fluids acts a constant and uniform gravitational field directed along the negative z-axis, g being the modulus of the corresponding acceleration.

A. Flow field around the bubble

The velocity potential in the liquid can be written in spherical coordinates by means of the well-known Legendre expansion:

$$\varphi(r, \mu; t) = \sum_{k=0}^{\infty} c_k(t) \frac{P_k(\mu)}{r^{k+1}} + \sum_{m=1}^{\infty} d_m(t) P_m(\mu) r^m. \tag{1}$$

In equation (1), μ is the cosine of the colatitude θ (along the z-axis, $\theta = 0$ for $z > z_{\mathrm{cm}}$, $\theta = \pi$ for $z < z_{\mathrm{cm}}$), P_l the lth Legendre polynomial and r is the distance from the origin. The potential is assumed as vanishing at infinity ($r \to \infty$), so that $d_m = 0$ for any m.

On the bubble boundary ($r = R$), the normal component of the velocity of the liquid (u_r) must take into account of the time derivative of the radius ($\dot{R}$) and the bubble translation velocity ($\dot{z}_{\mathrm{cm}}$), by means of the Neumann condition:

$$u_r[R(t), \mu; t] = \frac{\partial \varphi}{\partial r}[R(t), \mu; t] = \dot{R}(t) P_0(\mu) + \dot{z}_{\mathrm{cm}}(t) P_1(\mu).$$

It relates the above Legendre coefficients to the bubble motion in the following way:

$$c_0 = -R^2 \dot{R}, \qquad c_1 = -\frac{1}{2} R^3 \dot{z}_{\mathrm{cm}} \qquad c_k = 0 \ \text{ for } \ k \geq 2. \tag{2}$$

Moreover, on the same boundary the pressure on the gas/vapour face (p_{b}) is balanced by the pressure p acting on the liquid face and by the surface tension: $p_{\mathrm{b}} = p + 2\sigma/R$, where σ

is the surface tension coefficient of the gas-liquid interface. As a consequence, $p_{\rm b}$ is not uniform. It is expanded in the Legendre series:

$$\frac{p_{\rm b}}{\rho}(\mu;t) = \frac{\bar{p}_{\rm b}}{\rho}(t) + \sum_{k=1}^{\infty} \pi_k(t)\, P_k(\mu), \tag{3}$$

in which its mean value on the sphere $\bar{p}_{\rm b}$ is usually written as the sum of the constant vapour pressure $p_{\rm v}$ (at the ambient temperature) and the gas pressure $p_{\rm g}$, related to the bubble volume V by the isothermal equation of state:

$$p_{\rm g}(t)V(t) = p_{\rm g}(0)V(0). \tag{4}$$

The remaining Legendre coefficients π_k ($k \geq 1$) have to be calculated, as discussed below. Once the pressure-like quantity:

$$P(t) := \frac{\bar{p}_{\rm b}(t) - p_\infty}{\rho} + g z_{\rm cm}(t) - \frac{2\sigma}{\rho R(t)} \tag{5}$$

is introduced, the Legendre coefficients π_k for $k \geq 1$ (3) are related to the bubble motion by means of the Bernoulli law

$$-\frac{\partial \varphi}{\partial t} = \frac{|\boldsymbol{u}|^2}{2} + \frac{p - p_\infty}{\rho} + gz,$$

p_∞ being the asymptotic value assumed as $|\boldsymbol{x}| \to \infty$ by $p + \rho g z$. It follows:

$$\begin{aligned} -\frac{\dot{c}_0}{R}\, P_0 - \frac{c_0 \dot{z}_{\rm cm} + \dot{c}_1}{R^2}\, P_1 - \frac{2 c_1 \dot{z}_{\rm cm}}{R^3}\, P_2 = \\ = \left(\frac{1}{2}\,\frac{c_0^2}{R^4} + \frac{c_1^2}{R^6} + P\right) P_0 + \left(2\,\frac{c_0 c_1}{R^5} + gR + \pi_1\right) P_1 + \left(\frac{c_1^2}{R^6} + \pi_2\right) P_2 + \sum_{k=3}^{\infty} \pi_k P_k. \end{aligned} \tag{6}$$

B. Dynamics of radius and of center of mass of the bubble

The first consequence of relation (6) is that $\pi_k = 0$ for $k \geq 3$. Moreover, its projection along P_0 leads to the time evolution equation of the bubble radius:

$$\ddot{R} = \frac{1}{R}\left(-\frac{3}{2}\,\dot{R}^2 + \frac{1}{4}\,\dot{z}_{\rm cm}^2 + P\right). \tag{7}$$

The differential equation (7) being of the second order, the initial values of R, *i.e.* $R(0) := R_0$, and of its time derivative, *i.e.* $\dot{R}(0) := \dot{R}_0$, have to be prescribed.

The position of the center of mass of the bubble, $\boldsymbol{x}_{\rm cm}$, is written in terms of the density $\rho_{\rm b}$ of the gas/vapour mixture as:

$$\boldsymbol{x}_{\rm cm}(t) = \frac{1}{m_{\rm b}} \int_{V(t)} dV(\boldsymbol{x};t)\, \rho_{\rm b}(\boldsymbol{x};t)\, \boldsymbol{x},$$

$m_{\rm b} = \overline{\rho}_{\rm b} V$ being the constant mass of gas/vapour trapped inside the bubble. As a consequence, the mean density of the mixture changes according to the following equation:

$$\bar{\rho}_{\rm b}(t) V(t) = \bar{\rho}_{\rm b}(0) V(0). \tag{8}$$

The mixture moves according to the equation:

$$\rho_{\rm b} D_t \boldsymbol{u} = -\boldsymbol{\nabla} p_{\rm b} - \rho_{\rm b} g\, \boldsymbol{e}_z$$

and then the second time derivative of the position of the center of mass can be written as:

$$\ddot{\boldsymbol{x}}_{\rm cm} = \frac{1}{m_{\rm b}} \int_V dV\, \rho_{\rm b}\, D_t \boldsymbol{u} = -\frac{1}{m_{\rm b}} \int_{\partial V} dS\, p_{\rm b}\, \boldsymbol{n} - g \boldsymbol{e}_z. \tag{9}$$

The only nonvanishing component of the right-hand side is along the z-axis, so that if the initial position and velocity of the center of mass are prescribed along z, it turns out to be $\boldsymbol{x}_{\rm cm} \equiv (0, 0, z_{\rm cm})^{\rm T}$ at any successive time.

By using the balance of the normal stresses at the bubble interface and the Bernoulli law in the liquid, $p_{\rm b}$ is written as $p + 2\sigma/R$, that is

$$p_{\rm b} = p_\infty - \rho g z - \rho \left(\frac{\partial \varphi}{\partial t} + \frac{|\boldsymbol{u}|^2}{2} \right) + 2\, \frac{\sigma}{R},$$

so that the integral (9) can be evaluated. Note that it includes $\dot{c}_1$ which, in turn, depends on the acceleration $\ddot{z}_{\rm cm}$, as shown by the second relation (2). The resulting equation is

solved with respect to $\ddot{z}_{\rm cm}$ and, once the ratio between the mean gas/vapour and the liquid densities:

$$\varepsilon(t) := \frac{\bar{\rho}_{\rm b}(t)}{\rho} \tag{10}$$

has been introduced, the equation of motion of the center of mass of the bubble follows:

$$\ddot{z}_{\rm cm} = 2g\,\frac{1-\varepsilon}{1+2\,\varepsilon} - \frac{3}{1+2\,\varepsilon}\,\frac{\dot{R}}{R}\,\dot{z}_{\rm cm}. \tag{11}$$

This equation reduces to the one for the dynamics of a rigid sphere (see Batchelor, 1967, Equation 6.8.20) by enforcing $R \equiv$ constant, and to the equation for vertical motion in Tuteja *et al.* (2010) when taking $\varepsilon = 0$. As usual, the evolution equation (9) being of the second order, the position, *i.e.* $z_{\rm cm}(0) =: z_{\rm cm0}$, and the velocity, *i.e.* $\dot{z}_{\rm cm}(0) =: \dot{z}_{\rm cm0}$, of the center of mass at the initial time have to be assigned.

Finally, from the Bernoulli law (6) and from the dynamics of the center of mass (11) the two non-vanishing Legendre coefficients of the pressure $p_{\rm b}$ on the vapour/gas face of the bubble interface are obtained:

$$\pi_1 = \frac{3\varepsilon}{1+2\varepsilon}\,(\dot{R}\dot{z}_{\rm cm} - gR), \qquad \pi_2 = \frac{3}{4}\,\dot{z}_{\rm cm}^2. \tag{12}$$

On the basis of the above considerations, the motion of the bubble is defined by the solution of the nonlinear ODE system formed by the evolution equations of the radius (7) and of the position of the center of mass (11), together with the isothermal equation of state (4), the mass conservation (8) and the definitions of P (5) and of ε (10). In the present paper, this system is numerically integrated by means of a fourth order Runge-Kutta method. In the following section, the evaluation of the pressure disturbance due to the bubble motion is briefly described.

III. ACOUSTICS OF THE RISING SPHERICAL BUBBLE

The pressure perturbation $\mathscr{P}(\boldsymbol{x}_\mathrm{o};t)$ radiated from the rising bubble and received, at time t, by an observer placed at the point $\boldsymbol{x}_\mathrm{o} = (r_\mathrm{o}\cos\beta_\mathrm{o}, r_\mathrm{o}\sin\beta_\mathrm{o}, z_\mathrm{o})^\mathrm{T}$ outside the bubble (see Figure 1) is now evaluated. It results to be a function of the distance of the observer from the z-axis (r_o), of the difference $z_\mathrm{o} - z_\mathrm{cm} =: \zeta$ and of the time.

The distance of the observer position from any given point $\boldsymbol{x} = (R\sin\theta\cos\beta, R\sin\theta\sin\beta, z_\mathrm{cm} + R\cos\theta)^T$ of the bubble surface is:

$$|\boldsymbol{x}_\mathrm{o} - \boldsymbol{x}| = (R^2 - 2R\zeta\cos\theta + \zeta^2 + r_\mathrm{o}^2)^{1/2}[1 - \chi^2\cos(\beta - \beta_\mathrm{o})]^{1/2}, \tag{13}$$

with $\chi \in [0,1)$ given by

$$\chi^2 = \frac{2Rr_\mathrm{o}\sin\theta}{R^2 - 2R\zeta\cos\theta + \zeta^2 + r_\mathrm{o}^2}.$$

Note that $\chi \to 1$ as $r_\mathrm{o} \to R\sin\theta$ and $\zeta \to R\cos\theta$, *i.e.* for $\boldsymbol{x}_\mathrm{o}$ approaching the bubble surface.

The expression of the acoustic pressure disturbance can be written according to Ffowcs Williams and Hawkings (1969), neglecting the contribution of volume sources, that is including only the so-called *thickness* and *loading* terms. However, the form adopted here is a solution of the Ffowcs Williams and Hawkings equation derived by Farassat (2007), known as *formulation 1.* Along with symbols defined so far, one further introduces: $\boldsymbol{\xi} = \boldsymbol{x}_\mathrm{o} - \boldsymbol{x}$, $\xi = |\boldsymbol{\xi}|$, $u_\xi = \boldsymbol{u}\cdot\boldsymbol{\xi}/\xi$ (the component of bubble velocity along $\boldsymbol{\xi}$) and the source time, t_s. Farassat's formulation 1 can be written as:

$$\mathscr{P}(\boldsymbol{x}_{\mathrm{o}};t) = \frac{\rho}{4\pi}\frac{\partial}{\partial t}\int_{\partial V} dS \left[\frac{u_n}{\xi(1-u_\xi/c_\infty)}\right]_{t_{\mathrm{s}}=t_{\mathrm{e}}} + \frac{1}{4\pi c_\infty}\frac{\partial}{\partial t}\int_{\partial V} dS \left[\frac{p\,\boldsymbol{n}\cdot\boldsymbol{\xi}}{\xi^2(1-u_\xi/c_\infty)}\right]_{t_{\mathrm{s}}=t_{\mathrm{e}}} + \frac{1}{4\pi}\int_{\partial V} dS \left[\frac{p\,\boldsymbol{n}\cdot\boldsymbol{\xi}}{\xi^3(1-u_\xi/c_\infty)}\right]_{t_{\mathrm{s}}=t_{\mathrm{e}}}, \tag{14}$$

where c_∞ is the speed of sound in the undisturbed medium. Under the integral sign, $\boldsymbol{u}$, $\boldsymbol{n}$ (then u_n) and p are to be considered as funcions of $\boldsymbol{x}$ and t_{s}. Integration is performed on the surface of the bubble. The subscript $t_{\mathrm{s}} = t_{\mathrm{e}}$ means that values of integrands, at each point of the surface, are calculated at the proper *emission time*, determined through the solution of:

$$|\boldsymbol{x}_{\mathrm{o}} - \boldsymbol{x}(t_{\mathrm{e}})| = c_\infty(t - t_{\mathrm{e}}).$$

There is evidence that, in most cases, far-field acoustic pressure from bubbles or cavities is due to rapid oscillations of their volume. This is represented by the first term in equation (14). However, in order to have a clear picture of all the mechanisms at work in generating pressure disturbances from a moving bubble, it is instructive to look at the (very) near-field behaviour of the system. Here the wave equation is dominated by the Laplacian (Lezzi and Prosperetti, 1986): in fact, by letting $c_\infty \to \infty$ in equation (14), one obtains

$$\mathscr{P}(\boldsymbol{x}_{\mathrm{o}};t) = \frac{\rho}{4\pi}\frac{\partial}{\partial t}\int_{\partial V} dS(\boldsymbol{x};t_{\mathrm{s}})\,\frac{u_n(\boldsymbol{x};t_{\mathrm{s}})}{|\boldsymbol{x}_{\mathrm{s}}-\boldsymbol{x}|} + \frac{1}{4\pi}\int_{\partial V} dS(\boldsymbol{x};t_{\mathrm{s}})\,\tilde{p}(\boldsymbol{x};t_{\mathrm{s}})\,\boldsymbol{n}(\boldsymbol{x};t_{\mathrm{s}})\cdot\frac{\boldsymbol{x}_{\mathrm{o}}-\boldsymbol{x}}{|\boldsymbol{x}_{\mathrm{o}}-\boldsymbol{x}|^3}, \tag{15}$$

This means neglecting the time due to propagation of sound from the source to the observer, thus considering the system as *instantaneous*, rather than *retarded*. It seems

reasonable, thinking of the large speed of sound in water and the small source-observer distance for the case examined. In equation (15) the normal velocity u_n and the pressure $\tilde{p}$ at a point $\boldsymbol{x} \in \partial V$ are as follows

$$u_n = \dot{R} + \dot{z}_{\rm cm} \cos\theta, \qquad\qquad \tilde{p} = \pi_1 \cos\theta + \frac{3}{2}\,\pi_2 \cos^2\theta,$$

where π_1 and π_2 are given in equations (12). In fact, $\tilde{p}$ is the part of p, on the bubble surface, exceeding the uniform term

$$\frac{\bar{p}_{\rm b}}{\rho} - \frac{2\sigma}{\rho R} - \frac{\pi_2}{2},$$

which is going to give a vanishing contribution to the relevant integral in equation (15).

Using the distance (13) the pressure disturbance is evaluated in terms of the complete elliptic integrals of the first kind K and of the second kind E as:

$$\mathscr{P}(\boldsymbol{x}_{\rm o}; t) = \frac{\rho}{\pi}\,\frac{\partial}{\partial t}\left[R^2 \int_0^\pi d\theta\, \sin\theta\, \frac{\dot{R} + \dot{z}_{\rm cm}\cos\theta}{D}\, K(k)\right] + \frac{\rho R^2}{4\pi} \int_0^\pi d\theta\, \sin\theta\, \frac{\tilde{p}}{D} \left\{ \frac{4(\zeta\cos\theta - R)}{D^2}\, \frac{E(k)}{k'^2} + \frac{1}{R}\left[\frac{2-k^2}{k'^2}\, E(k) - 2K(k)\right]\right\}. \quad (16)$$

In equation (16) the quantity

$$D := \left[(r_{\rm o} + R\sin\theta)^2 + (\zeta - R\cos\theta)^2\right]^{1/2}$$

has been introduced for short. Moreover, the modulus of the elliptic integral is:

$$k = \frac{2\sqrt{R r_{\rm o} \sin\theta}}{D}. \quad (17)$$

and the complementary modulus is $k' = (1 - k^2)^{1/2}$.

In the general case in which the observer does not lie on the z-axis ($r_{\rm o} > 0$), $\mathscr{P}$ is evaluated by deriving in time inside the integral (16) and then performing a numerical

integration. This latter is not needed for $r_\mathrm{o} = 0$ (observer lying on the z-axis), that implies $k = 0$ by means of the definition of the modulus (17). Due to the fact that $K(0) = \pi/2$, the pressure perturbation $\mathscr{P}$ (16) takes the form:

$$\mathscr{P}(\boldsymbol{x}_\mathrm{o}; t) = \frac{\rho}{3}\frac{R^3}{|\zeta|}\left(3\,\frac{\ddot{R}}{R} + 6\,\frac{\dot{R}^2}{R^2} + \frac{6}{\zeta}\,\frac{\dot{R}}{R}\,\dot{z}_\mathrm{cm} + \frac{1}{\zeta}\,\ddot{z}_\mathrm{cm} + \frac{2}{\zeta^2}\,\dot{z}_\mathrm{cm}^2 + \frac{1}{\zeta}\,\frac{\pi_1}{R} + \frac{6}{5\zeta^2}\,\pi_2\right). \tag{18}$$

In the following results, the integral (16) is not used to calculate the pressure perturbation from the rising bubble. In fact, it can be successfully replaced by an approximation (named as $\mathscr{P}^\mathrm{a}$), that is obtained by neglecting powers of order greater than 3 of the ratio $\eta = R/\delta_\mathrm{o}$, δ_o being the distance of the observer from the center of mass of the bubble, *i.e.*, $\delta_\mathrm{o} = (r_\mathrm{o}^2 + \zeta^2)^{1/2}$. Using appropriate Maclaurin expansions for powers of:

$$\frac{1}{|\boldsymbol{x}_\mathrm{o} - \boldsymbol{x}|} = \frac{1}{\delta_\mathrm{o}}\left\{1 - 2\,\frac{R}{\delta_\mathrm{o}}\left[\frac{\zeta}{\delta_\mathrm{o}}\,\cos\theta + \frac{r_\mathrm{o}}{\delta_\mathrm{o}}\,\sin\theta\cos(\beta - \beta_\mathrm{o})\right] + \frac{R^2}{\delta_\mathrm{o}^2}\right\}^{1/2} := \frac{1}{\delta_\mathrm{o}}\left(1 - 2\eta\gamma + \eta^2\right),$$

in the parameter $-2\eta\gamma + \eta^2$, the pressure perturbation (15) is approximated by:

$$\mathscr{P}^\mathrm{a}(\boldsymbol{x}_\mathrm{o}; t) = \frac{\rho}{3}\frac{R^3}{\delta_\mathrm{o}}\left[3\,\frac{\ddot{R}}{R} + 6\,\frac{\dot{R}^2}{R^2} + \frac{6\zeta}{\delta_\mathrm{o}^2}\frac{\dot{R}}{R}\,\dot{z}_\mathrm{cm} + \frac{\zeta}{\delta_\mathrm{o}^2}\,\ddot{z}_\mathrm{cm} + \frac{1}{\delta_\mathrm{o}^2}\left(\frac{3\zeta^2}{\delta_\mathrm{o}^2} - 1\right)\dot{z}_\mathrm{cm}^2 + \frac{\zeta}{\delta_\mathrm{o}^2}\,\frac{\pi_1}{R} + \frac{3}{5\delta_\mathrm{o}^2}\left(\frac{3\zeta^2}{\delta_\mathrm{o}^2} - 1\right)\pi_2\right]. \tag{19}$$

On the symmetry axis ($r_\mathrm{o} = 0$, $\delta_\mathrm{o} = |\zeta|$) the approximation (19) gives the exact representation (18).

The first five terms of equation (19) are generated by the first integral in the right-hand side of equation (15). This would give rise in the far field to the so-called *thickness noise*, and is related to the geometry and kinematic properties of the moving source. The first three terms, containing time derivatives of bubble radius, are responsible for the *monopole* character of the far-field noise of the bubble. The fourth and fifth terms

of equation (19), contain only derivatives of position of the center of mass of the bubble. They clearly exhibit a different directivity pattern and a higher order dependence on the inverse of the source-observer distance, which gives them a dipole character. In fact, they share the structure of the last two terms of equation (19), generated by the second integral in the right-hand side of equation (15). These, coming from bubble surface pressure loading, are widely known as *dipole* terms. As it will be seen from the illustration of some sample results, they give a smaller contribution compared to the corresponding terms from thickness, affecting the absolute value of the peak disturbance, while not changing the overall pattern.

Moving to the far field, the complete right-hand side of equation (14) should be considered. However, it is clear from the previous analysis the growing dominance of thickness terms from bubble radius (that is, volume) oscillation. As far as the second integral in the right-hand side of equation (14) is concerned, one may observe that it is still affected by the dependence on c_∞^{-1}. This results in a limited contribution to the overall signal, compared to that generated by the first integral, at least in the generality of cases. Particular situations, where it may be comparable to (or even dominant on) thickness noise, may be caused by different patterns of bubble dynamics. One such case may be given when rapid oscillations of surface pressure load are generated independently of the radius pulsation, as in the interaction of bubble with unsteady vortex motion. A further example is that provided in the case of phenomena causing intense shock waves to be released by the collapse of a bubble in the vicinity of a solid surface, as it was shown in a previous application of Ffowcs Williams and Hawkings formulation to bubble acoustics (Jamaluddin *et al.*, 2011).

IV. NUMERICAL RESULTS

All the quantities are made nondimensional by adopting the initial bubble radius R_0 as scale of lengths, ρR_0^3 as scale of masses and the quantity $T_0 = 2\pi/\omega_0$ as scale of times, where ω_0 is the natural (circular) frequency of oscillation of the bubble, given as ω_N by Brennen (1995). There, the definition of ω_N is based on the *equilibrium radius* (the value of R for a bubble with a given amount of gas to be in equilibrium at the given condition of external pressure), while ω_0 is calculated here using R_0, which is made the equilibrium radius at the given external pressure by properly choosing the amount of gas contained in the bubble. In the present calculations the bubble contains air at temperature 20 °C, moves in water by starting with radius $R_0 = 2$ mm and center of mass in $z_{\rm cm} = -0.1$ m, so that T_0 results to be less than 1 ms. The surface tension coefficient σ at the bubble wall is 0.0729 N m^{-1}. In the following discussion, the symbols introduced so far to denote the dimensional quantities will be used for the corresponding nondimensional quantities, while, for the sake of clarity, initial data will be presented in dimensional form.

The main feature of the proposed model for the motion of the center of mass of the bubble and its consequences on the pressure perturbation are illustrated in Figures 2 and 3.

Neglecting gas density inside the bubble, that is enforcing $\varepsilon = 0$, appears to be a common practice in most previous papers referenced here (in particular, in Tuteja *et al.*, 2010), which use the Lagrangian formulation to derive the equations of motion. This causes significant differences in the peak values of $\dot{z}_{\rm cm}$ (Fig. 2(a)), and results in an overestimation of the vertical position of the center of mass at a given time (Fig. 2(b)). Although this difference may be considered as a negligible one, the overall effect on the

pressure perturbation is surprisingly significant. At the observer position considered here, the peak amplitudes exhibit a difference of around 20% (Fig. 3), and also a slight phase shift between two corresponding peaks appears (magnified in the zoomed view).

Next issue is looking at how the model reproduces the main features of bubble dynamics. Figure 4 shows the starting evolution of a bubble with initial velocities $\dot{R}_0 = 5\ \mathrm{m\,s^{-1}}$ and $\dot{z}_{\mathrm{cm}0} = 0\ \mathrm{m\,s^{-1}}$. Typically, at the strong collapses of R (a) correspond large spikes in $\dot{z}$ (b), causing the stepped trend of z (c), characteristic of the bubble rising motion.

In order to take a global look at the system behaviour, a case with a different combination of initial data is studied next. Fig. 5 shows radial and vertical motions of a bubble starting with zero radial velocity and nonzero vertical velocity. These are compared with the analogous motions consequent to zero radial and zero vertical initial velocities, *i.e.* driven only by the effect of gravity. The latter curves are very smooth: they represent the rising motion, due to gravity, of a sphere steadily expanding because of the decreasing pressure along the rising path. The initial nonzero vertical velocity induces in the curve of the corresponding radial motion, shown in Fig. 5(a), an oscillating pattern around a global trend representing the steady expansion already observed in the curve of the motion with $\dot{z}_{\mathrm{cm}0} = 0\ \mathrm{m\,s^{-1}}$. The oscillation in this case is quite regular, and does not exhibit the violent collapse appearing in the pattern of Fig. 4, so that the curve in Fig. 5(b), showing the vertical motion of the center of mass, is not stepped: indeed it appears as smooth as the one of the vertical motion with $\dot{z}_{\mathrm{cm}0} = 0\ \mathrm{m\,s^{-1}}$.

Fig. 6 shows the pressure disturbance generated by the motion of the bubble at an observer position whose minimum distance from the moving source is 5 times the initial

bubble radius R_0. The signature generated by the motion with $\dot{z}_{\mathrm{cm}0} = 0$ m s^{-1} is smooth and closely resembles the acoustic time signature of a dipole source, like the one expected as the effect of a rigid body having a relative motion with respect to the observer. This is basically represented by the last two terms in equation (19), those depending on $\ddot{z}_{\mathrm{cm}}$ and $\dot{z}^2_{\mathrm{cm}}$. On the other hand, the signature generated by the motion with nonzero initial vertical velocity is clearly characterized by the oscillating pattern of the corresponding radial motion: it exhibits a significant monopole component, represented in equation (19) by terms containing time derivatives of R. This is superimposed to a dipole pattern similar to that of the curve with zero initial vertical velocity, although hidden by the large oscillations amplitude.

To better understand the combination of different effects in the resulting acoustic disturbance of the bubble, the signatures are filtered in time by calculating the average, $\mathscr{P}^{\mathrm{a}}_{\mathrm{ave}}$, and the root mean square, $\mathscr{P}^{\mathrm{a}}_{\mathrm{rms}}$ (with respect to $\mathscr{P}^{\mathrm{a}}_{\mathrm{ave}}$), of the function $\mathscr{P}^{\mathrm{a}}$ (De Bernardis and Riccardi, 2015). Thus, one finally gets:

$$\mathscr{P}^{\mathrm{a}}_{\mathrm{ave}}(t) := \frac{1}{T}\int_{-T/2}^{T/2} d\tau\, \mathscr{P}^{\mathrm{a}}(t+\tau),$$

$$\mathscr{P}^{\mathrm{a}}_{\mathrm{rms}}(t) := \sqrt{\frac{1}{T}\int_{-T/2}^{T/2} d\tau\, [\mathscr{P}^{\mathrm{a}}(t+\tau) - \mathscr{P}^{\mathrm{a}}_{\mathrm{ave}}(t)]^2}$$

(the dependencies on $\boldsymbol{x}_{\mathrm{o}}$ have been omitted, for the sake of shortness). Here T is, in principle, an arbitrary time interval. In practice, it is chosen as the time interval corresponding to an integer number of complete oscillations. This results in the curves drawn in Figs. 7 and 8. Fig. 7 shows the average curves of the pressure signatures pictured in Fig. 6. The curve with $\dot{z}_{\mathrm{cm}0} = 0$ m s^{-1} almost reproduces the original pressure

perturbation, saying that the averaging process is, more or less, uneffective in this case. On the contrary, the curve with $\dot{z}_{\mathrm{cm}0} = 0.5\ \mathrm{m\,s^{-1}}$ looks now very similar to the other one. The averaging process has removed the oscillating part of the signal, revealing the dipole-like carrier signature. Fig. 8 shows the root mean square curves of the pressure perturbation in Fig. 6. They are associated to the amplitude of the oscillations that have to be superimposed to the average curves in Fig. 7 in order to give back the pressure perturbation of Fig. 6. Finally, only for the case with $\dot{z}_{\mathrm{cm}0} = 0.5\ \mathrm{m\,s^{-1}}$, the pressure perturbation and the corresponding average and root mean square curves are reported in Fig. 9.

Equation (19) exhibits significant features. In fact, it describes the pressure disturbance generated by the bubble through the sum of several terms, each representing the role played in this phenomenon by a particular quantity related to the bubble dynamics. In particular, the first three terms, all including derivatives of R, represent the energy associated to the bubble pulsation, clearly exhibiting a monopole character. The last four terms (two including only derivatives of z_{cm}, two including components of the bubble surface pressure), show the dipole nature of the perturbation generated by a rigid body through its relative motion with respect to a steady observer. These two main components of equation (19) are separately drawn in Fig. 10, for the pressure perturbations of Fig. 9. In particular, one can observe that the second (dipole) part is very close to the average curve of the overall signature, as it is shown in Fig. 11. Here the dipole contributions from *thickness* (terms with derivatives of z_{cm}) and *loading* (terms with components of pressure) are plotted separately to show the relative magnitude.

Finally, Fig. 12 shows the result obtained in the calculation of the far-field acoustic signature of a rising bubble. It refers to the only (to authors' knowledge) available

experimental result for a single rising bubble in free space, so that it makes sense to have a true far-field prediction.

The experiment, reported in Strasberg (1956), performs measurement of sound generated by an air bubble released at a nozzle in water, next freely rising to gravity. The reference picture (not reproduced here) shows, along with the measured pressure, the shape of the rising bubble corresponding to selected times. Proper initial conditions for the integration procedure are derived from the experimental set-up, following suggestions given in the paper.

Because of the large distance of the observer, this comparison is not particularly suitable to highlight the features of the formulation presented here. In fact, in this case the acoustic signature could have been calculated considering just the *monopole thickness* (first three) terms in equation (19), using the correction to properly include retarded times, after correcting for compressibility effect also the dynamic equations. The remaining four (*dipole*) terms provide negligible contribution.

However, the comparison would show a reasonable agreement with the measured signature, with a 18% underestimation of the measured peak sound pressure (in the paper, the calculated 40% overestimation is claimed as "*... in fair agreement ...*"!), and a slower decay in the amplitude of the calculated waveform compared to the data. The departure from the measured peak pressure may be partly related to the uncertainty in extracting data from the picture of the measurement. If one looks at the picture, showing the evolution of the bubble shape, it is a reasonable hypothesis to relate the underestimation of the waveform decay to the constraint of spherical shape enforced in the mathematical model.

V. CONCLUDING REMARKS AND PERSPECTIVES

Main purpose of this work is the qualitative investigation of the acoustic disturbance radiated by a spherical bubble rising under the effect of the gravity through an inviscid isochoric fluid. A modified Rayleigh-Plesset (RP) equation for the bubble radius has been introduced, together with an equation for the dynamics of the center of mass of the bubble. These equations exhibit a twofold nonlinear coupling. The equation for the radial motion, compared to the original form of the RP equation for a pulsating bubble at rest in an inviscid fluid, includes an additional term that is proportional to the kinetic energy of the translating motion. Equation (11) describing the motion of the center o mass is a general representation of a translating bubble with time-varying radius and is coupled to the RP equation through a mixed term containing the product $\dot{R}\dot{z}_{\rm cm}$. It includes, as particular cases, the equation for the vertical motion of a rigid sphere ($R \equiv$ constant) (Batchelor, 1967), as well as the equation for the rising motion of a bubble proposed by Tuteja *et al.* (2010).

It is worth noticing that in the extensive literature summarized in the Introduction, mostly based on the Lagrangian formulation for the derivation of the equations of motion, it is a common practice to neglect the ratio ε between the density of the mixture inside the bubble and the one of the external liquid. It has been shown here that it may significantly affect the pressure disturbance, in particular when the bubble motion leads to large volume variations.

A further remark concerns the closed form (19), proposed for estimating the acoustic signature radiated by the rising bubble. It was already observed that this formula allows

for the qualitative understanding of the roles played by velocities and accelerations in the acoustic emission of the rising bubble. One more feature has been actually shown here: formula (19) separates monopole and dipole contributions, and these components appear to be closely related to the root mean square and average, respectively, of the acoustic signature. Although the formula was derived to propose a qualitative study of the bubble pressure disturbance in the near field, it has been successfully used, properly adapted along with the dynamic equations, to simulate the pressure signature measured in a laboratory experiment.

The results of the numerical integration of the system of equations for the dynamics of the rising bubble have been successfully compared with those of a three-dimensional boundary element code, which simulates the potential flow in the liquid. In the near future, this code will be used for investigating the departures of the bubble shape from the spherical one during the rising, as well as for estimating their effects on the acoustics. Furthermore, it will be used to study the dynamics, and thereby generated sound, of a non-spherical rising bubble. Analytical and numerical extensions of the present approach to the bubble rising in presence of a wall or of a (fixed) free surface are also under investigation at the present time.

Acknowledgements

Activities described here were conducted under Grant of the Flagship Project *RITMARE* — The Italian Research for the Sea — coordinated by the National Research Council of Italy, funded by the Ministry of Education, University and Research within the National Research Programme 2011-2013.

REFERENCES

Batchelor, G. K. (**1967**), *An Introduction to Fluid Dynamics* (Cambridge University Press, Cambridge).

Brennen, C. E. (**1995**), *Cavitation and Bubble Dynamics* (Oxford University Press, Oxford).

Ceccio, S. L. and Brennen, C. E. (**1991**), "Observations of the dynamics and acoustics of travelling bubble cavitation," J. Fluid Mech. **233**, 633–660.

Chakraborty, B. B. (**1990**), "Effect of a viscous fluid flow past a spherical gas bubble on the growth of its radius," Proc. Indian Acad. Sci. (Math. Sci.) **10**(2), 185–188.

Chakraborty, B. B. and Tuteja, G. S. (**1993**), "Motion of an expanding, spherical gas bubble in a viscous liquid under gravity," Phys. Fluids **5**(8), 1879–1882.

Chang, N. A. and Ceccio, S. L. (**2011**), "The acoustic emissions of cavitation bubbles in stretched vortices," J. Acoust. Soc. Am. **130**(5), 3209–3219.

Choi, J. and Ceccio, S. L. (**2007**), "Dynamics and noise emission of vortex cavitation bubbles," J. Fluid Mech. **575**, 1–26.

De Bernardis, E. and Riccardi, G. (**2015**), "Acoustics of a bubble rising in a gravitational field," in *CD ROM Proc. 22nd International Congress on Sound and Vibration* (Florence, Italy, 12-16 July 2015), ISBN 978-88-88942-48-3.

Doinikov, A. A. (**2002**), "Translational motion of a spherical bubble in an acoustic standing wave of high intensity," Phys. Fluids **14**(4), 1420–1425.

435 Doinikov, A. A. (**2004**), "Translational motion of a bubble undergoing shape oscillations,"
436 J. Fluid Mech. **501**, 1–24.

437 Farassat, F. (**2007**), "Derivation of formulations 1 and 1A of Farassat," Tech. Rep.
438 TM-2007-214853, NASA.

439 Ffowcs Williams, J. E. and Hawkings, D. L. (**1969**), "Sound Generation by Turbulence and
440 Surfaces in Arbitrary Motion," Phil. Trans. R. Soc. Lond. A **264**, 321–342.

441 Gordillo, J. M., Lalanne, B., Risso, F., Legendre, D., and Tanguy, S. (**2012**), "Unsteady
442 rising of clean bubble in low viscosity liquid," Bubble Science, Engineering and
443 Technology **4**(1), 4–11.

444 Jamaluddin, A. R., Ball, G. J., Turangan, C. K., and Leighton, T. G. (**2011**), "The
445 collapse of single bubbles and approximation of the far-field acoustic emissions for
446 cavitation induced by shock wave lithotripsy," J. Fluid Mech. **677**, 305–341.

447 Keller, J. B. and Miksis, M. (**1980**), "Bubble oscillations of large amplitude," J. Acoust.
448 Soc. Am. **68**(2), 628–633.

449 Klaseboer, E. and Khoo, B. C. (**2006**), "A modified Rayleigh-Plesset model for a
450 non-spherically symmetric oscillating bubble with applications to boundary integral
451 methods," Eng. Anal. Bound. Elem. **30**, 59–71.

452 Leighton, T. G. (**1994**), *The Acoustic Bubble* (Academic Press, London).

453 Lezzi, A. and Prosperetti, A. (**1986**), "Bubble dynamics in a compressible liquid. Part 2.
454 Second order theory," J. Fluid Mech. **185**, 289–321.

455 Magnaudet, J. and Legendre, D. (**1998**), "The viscous drag force on a spherical bubble
456 with a time-dependent radius," Phys. Fluids **10**(3), 550–554.

457 Plesset, M. S. (**1954**), "On the stability of fluid flows with spherical symmetry," J. Appl.
458 Phys. **25**(1), 96–98.

459 Reddy, A. J. and Szeri, A. J. (**2002**a), "Coupled dynamics of translation and collapse of
460 acoustically driven microbubbles," J. Acoust. Soc. Am. **112**(4), 1346–1352.

461 Reddy, A. J. and Szeri, A. J. (**2002**b), "Shape stability of unsteadily translating bubbles,"
462 Phys. Fluids **14**(7), 2216–2224.

463 Shaw, S. J. (**2006**), "Translation and oscillation of a bubble under axisymmetric
464 deformation," Phys. Fluids **18**(072104).

465 Strasberg, M. (**1956**), "Gas bubbles as sources of sound in liquids," J. Acoust. Soc. Am.
466 **28**(1), 20–26.

467 Tuteja, G. S., Khattar, D., Chakraborty, B. B., and Bansal, S. (**2010**), "Study of an
468 expanding, spherical gas bubble in a liquid under gravity when the centre moves in a
469 vertical plane," Int. J. Contemp. Math. Sciences **5**(22), 1065–1075.

470 Yang, B., Prosperetti, A., and Takagi, S. (**2003**), "The transient rise of a bubble subject to
471 shape or volume changes," Phys. Fluids **15**(9), 2640–2648.

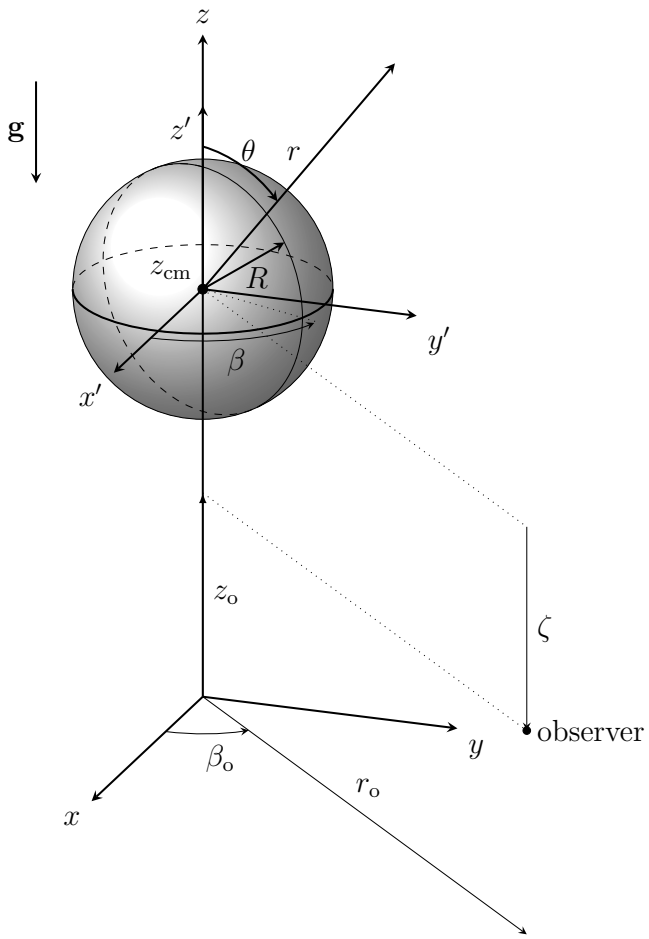

Figure 1: Schematic for bubble dynamics and acoustics.

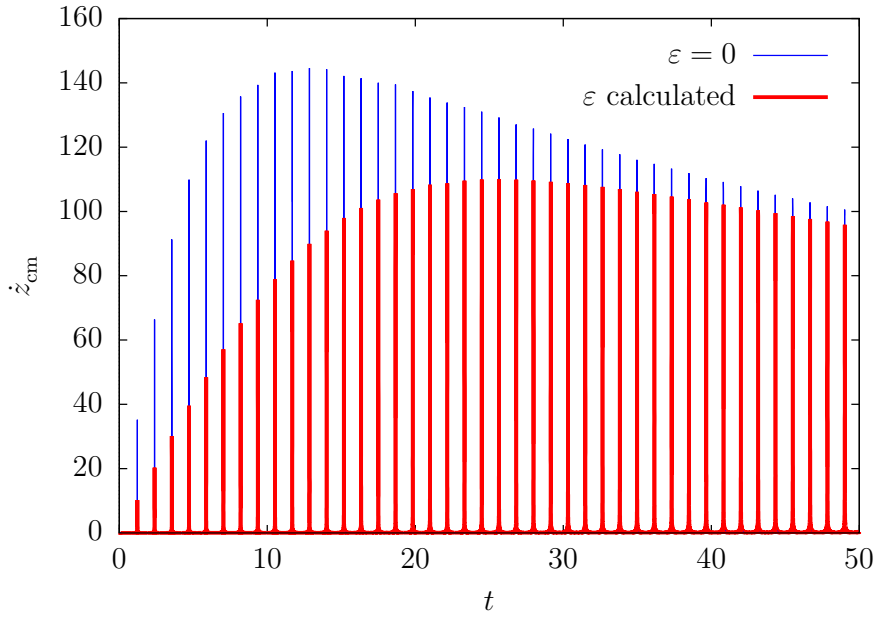

(a)

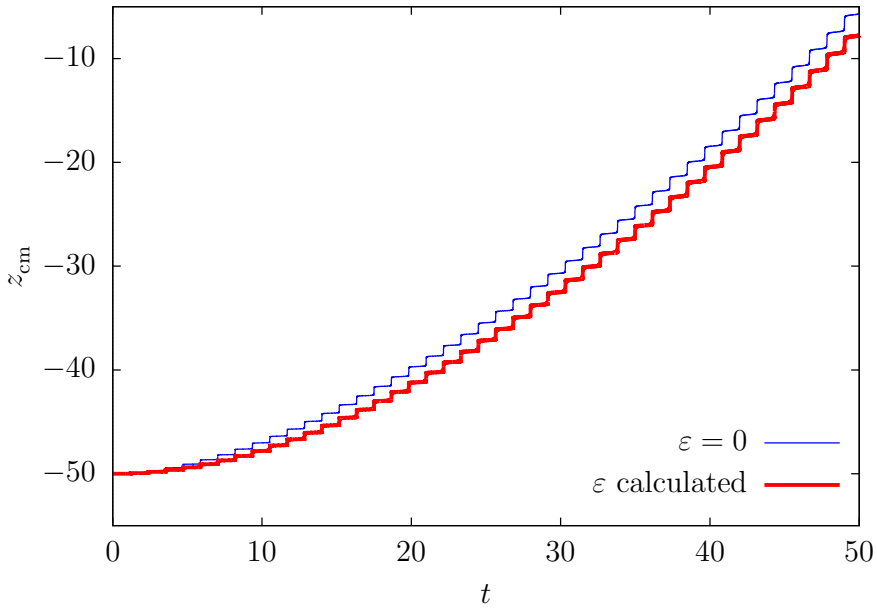

(b)

Figure 2: (Color online) Velocity (a) and position of the center of mass (b) of the bubble with density ratio ε calculated or enforced as $\varepsilon = 0$. Initial data: $\dot{R}_0 = 20\ \mathrm{m\,s^{-1}}$, $z_{\rm cm0} = -0.1$ m, $\dot{z}_{\rm cm0} = 0\ \mathrm{m\,s^{-1}}$.

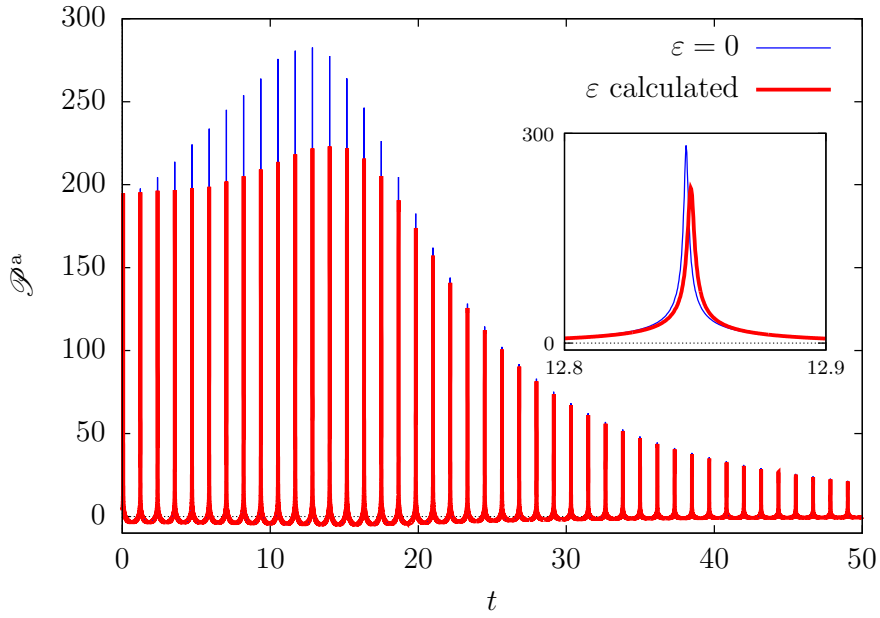

Figure 3: (Color online) Pressure disturbance, and zoom view of a relevant peak for the bubble with vertical motion represented in Fig. 2. The observer is at a distance $r_o = 0.01$ m from the bubble path.

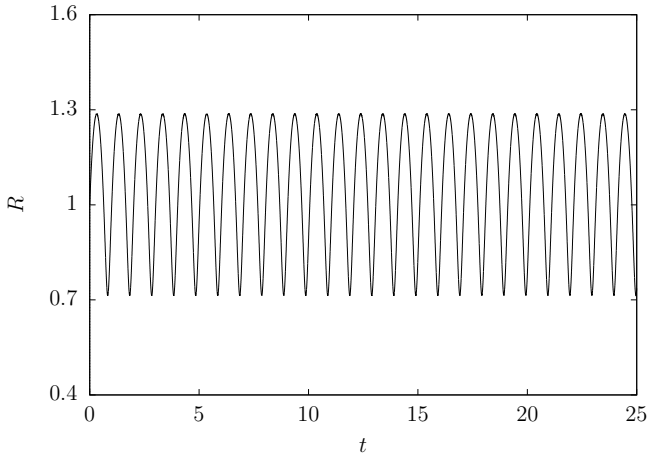

(a)

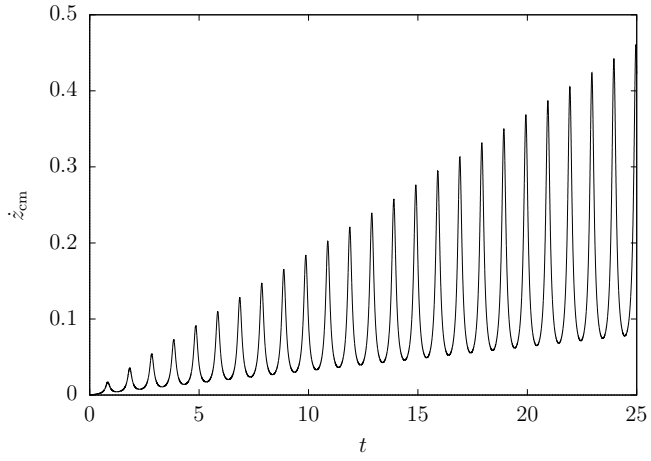

(b)

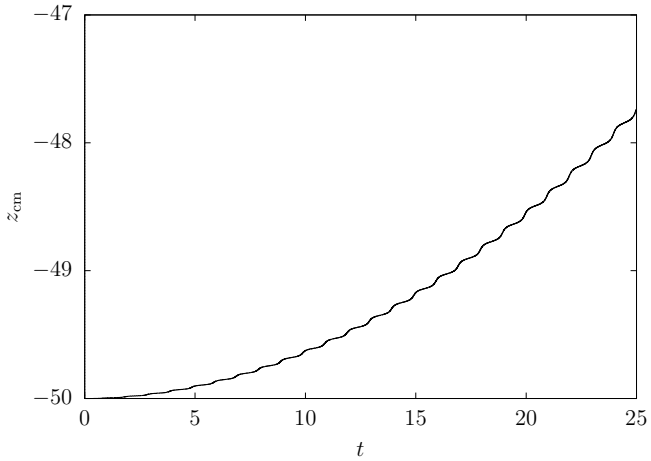

(c)

Figure 4: Bubble radius (a), center of mass velocity (b) and position (c). Initial data: $\dot{R}_0 = 5\ \mathrm{m\,s^{-1}}$, $\dot{z}_{\mathrm{cm}0} = 0\ \mathrm{m\,s^{-1}}$.

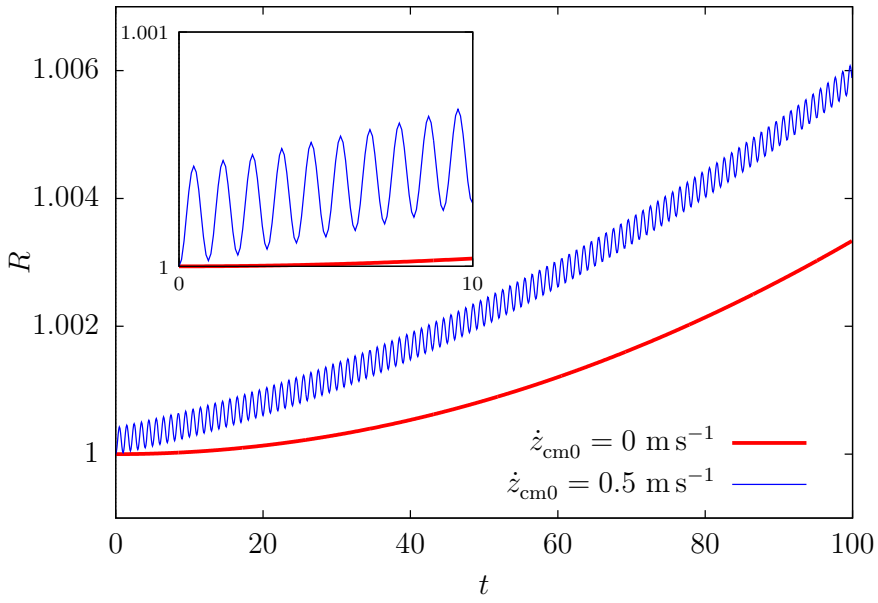

(a)

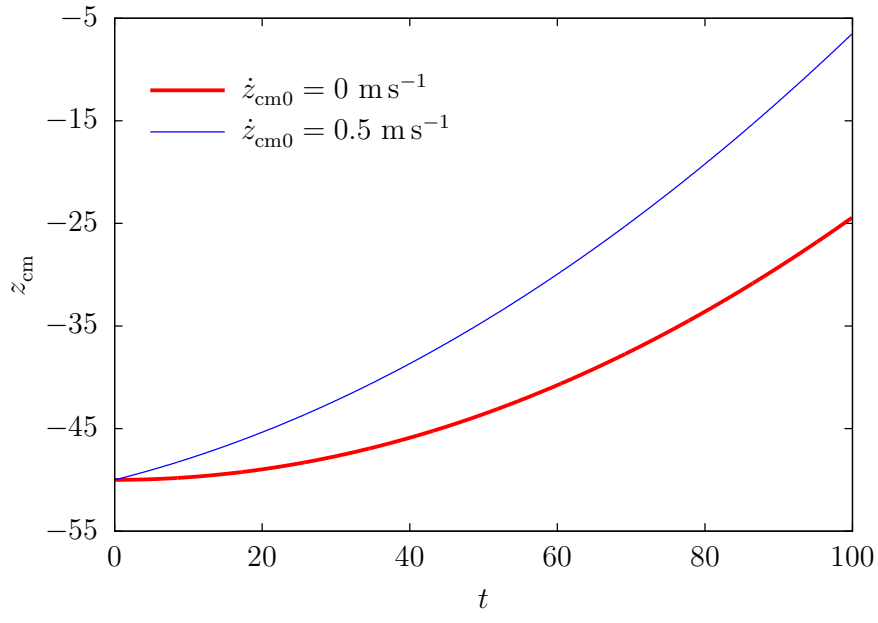

(b)

Figure 5: (Color online) Bubble radius (a) and center of mass position (b). Initial data: $\dot{R}_0 = 0$ m s^{-1}, $\dot{z}_{\rm cm0} = 0.5$ m s^{-1} and $\dot{z}_{\rm cm0} = 0$ m s^{-1}.

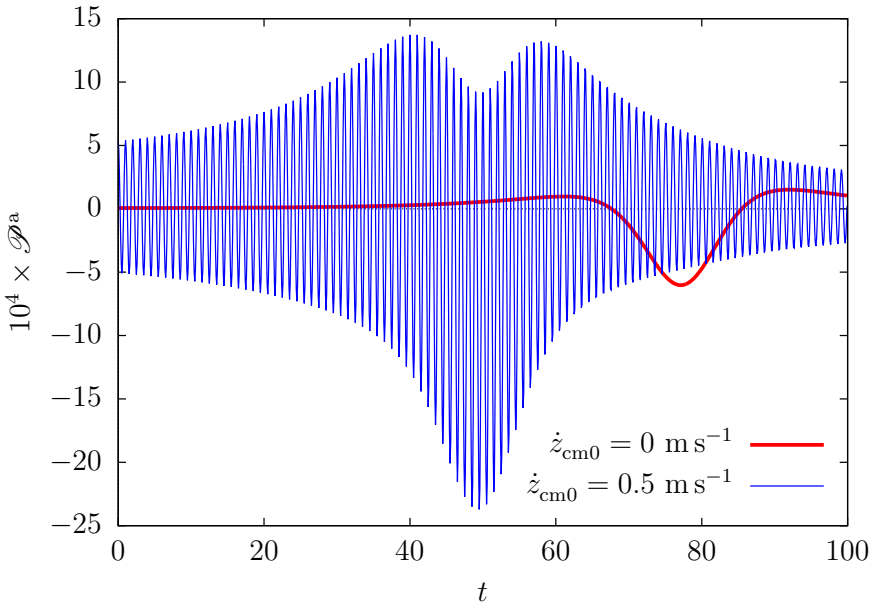

Figure 6: (Color online) Pressure disturbance for the bubble whose motions are shown in Fig. 5. The observer is at a distance $r_{\mathrm{o}} = 0.01$ m from the bubble path.

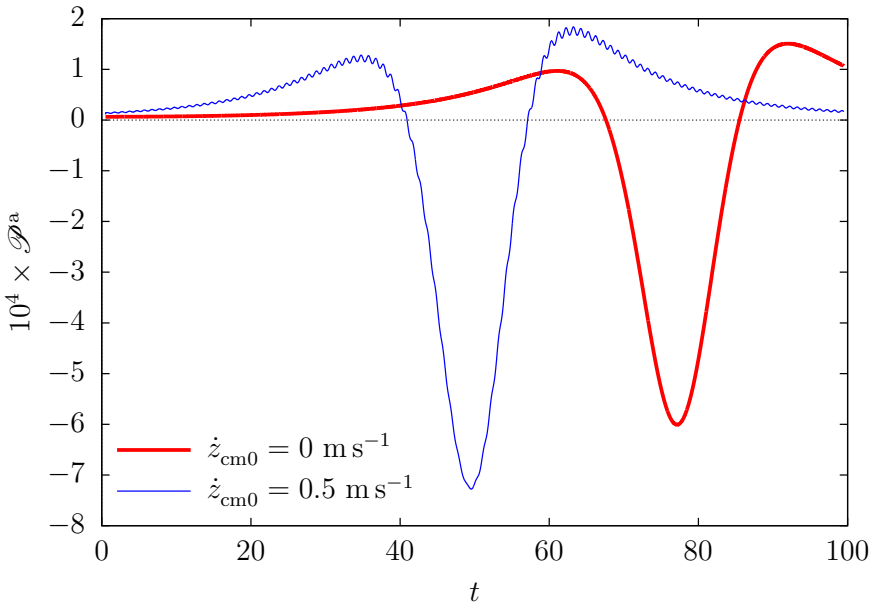

Figure 7: (Color online) Average curves of the pressure disturbances shown in Fig. 6.

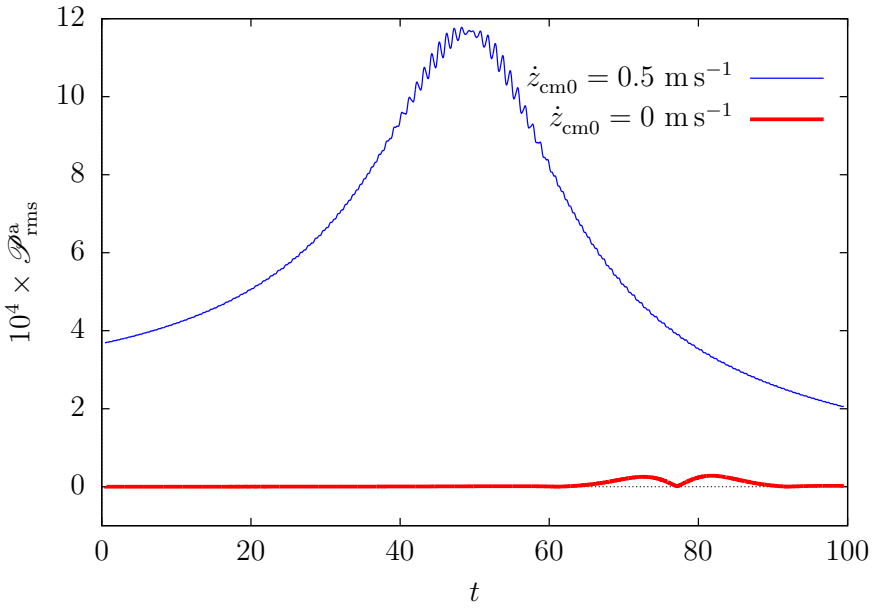

Figure 8: (Color online) Root mean square curves of the pressure disturbances shown in Fig. 6.

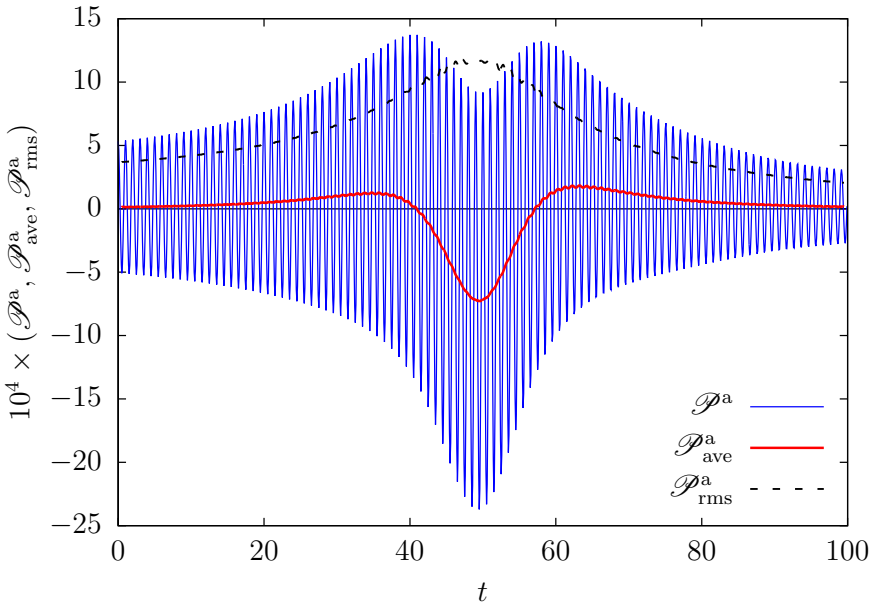

Figure 9: (Color online) Pressure disturbances shown in Fig. 6, and corresponding average and root mean square curves.

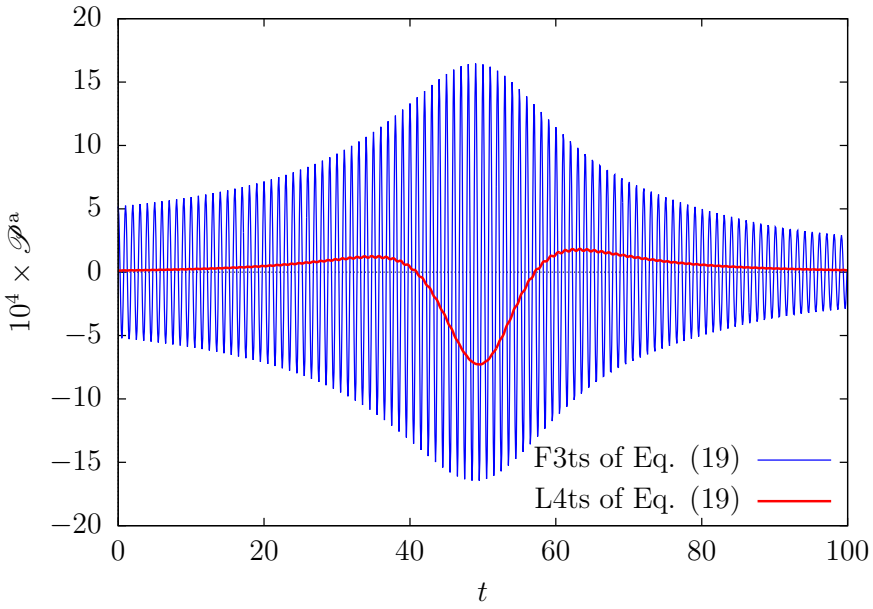

Figure 10: (Color online) Curve of the pressure disturbances, for the bubble whose motions are shown in Fig. 5 (with $\dot{z}_{\mathrm{cm0}} = 0.5\ \mathrm{m\,s^{-1}}$), calculated using the first three terms (F3ts) or the last two terms (L4ts) of equation (19).

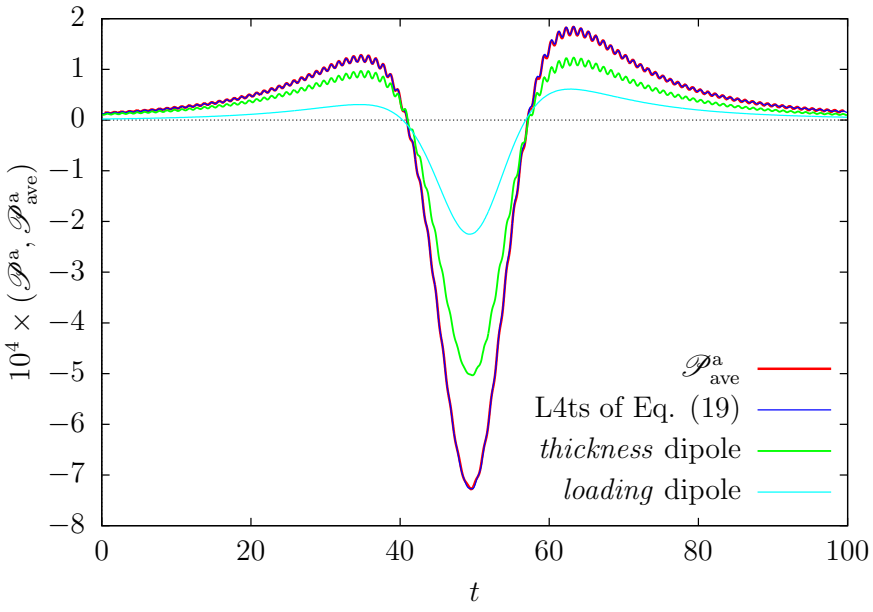

Figure 11: (Color online) Pressure disturbance calculated using the last four terms (L4ts) of equation (19) and average curve of the overall signature, for the bubble whose motions are shown in Fig. 5 (with $\dot{z}_{\rm cm0} = 0.5\ {\rm m\,s^{-1}}$). The former is the sum of *thickness* and *loading* dipole terms. These contributions are also plotted.

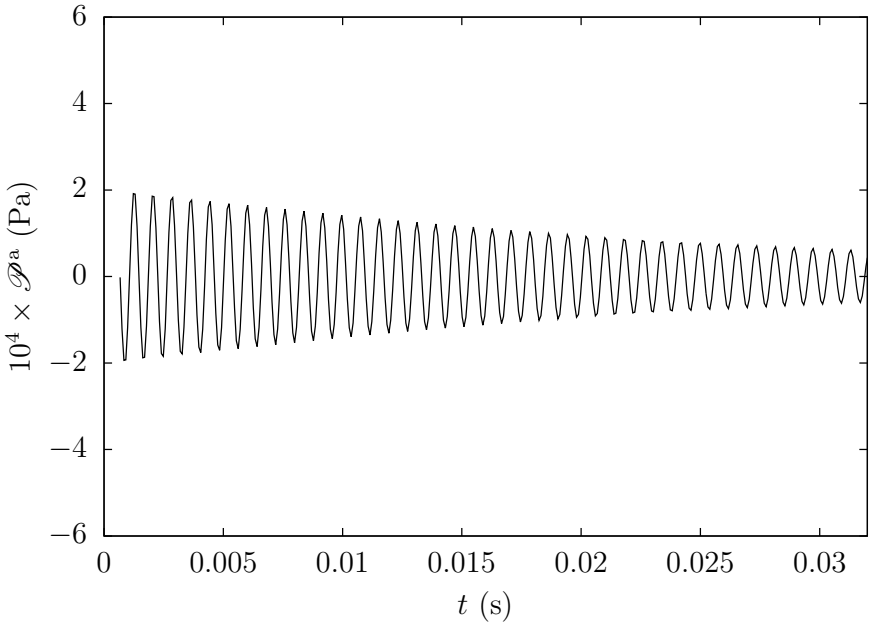

Figure 12: Far-field acoustic signature calculated using thickness noise only to compare with experimental acoustic signature for a single rising bubble reported in Strasberg (1956). Quantities in this figure are given in dimensional form.